Anal Bioanal Chem (2007) 387:1759–1767
DOI 10.1007/s00216-006-1079-9

ORIGINAL PAPER

Continuous nondestructive monitoring of *Bordetella pertussis* biofilms by Fourier transform infrared spectroscopy and other corroborative techniques

Diego Serra · Alejandra Bosch · Daniela M. Russo · María E. Rodríguez · Ángeles Zorreguieta · Juergen Schmitt · Dieter Naumann · Osvaldo Yantorno

Received: 7 July 2006 / Revised: 4 December 2006 / Accepted: 6 December 2006 / Published online: 10 January 2007

Abstract This work describes the application of several analytical techniques to characterize the development of *Bordetella pertussis* biofilms and to examine, in particular, the contribution of virulence factors in this development. Growth of surface-attached virulent and avirulent *B. pertussis* strains was monitored in continuous-flow chambers by techniques such as the crystal violet method, and nondestructive methodologies like fluorescence microscopy and Fourier transform (FT) IR spectroscopy. Additionally, *B. pertussis* virulent and avirulent strains expressing green fluorescent protein were grown adhered to the base of a glass chamber of 1-μm thickness. Three-dimensional images of mature biofilms, acquired by confocal laser scanning microscopy, were quantitatively analysed by means of the computer program COMSTAT. Our results indicate that only the virulent (Bvg^+) phase of *B. pertussis* is able to attach to surfaces and develop a mature biofilm. In the virulent phase these bacteria are capable of producing a biofilm consisting of microcolonies of approximately 200 μm in diameter and 24 μm in depth. FTIR spectroscopy allowed us not only to follow the dynamics of biofilm growth through specific biomass and biofilm marker absorption bands, but also to monitor the maturation of the biofilm by means of the increase of the carbohydrate-to-protein ratio.

Keywords *Bordetella pertussis* · Biofilm structure · Image analysis · Quantification · Fourier transform IR spectroscopy

D. Serra · A. Bosch · M. E. Rodríguez · O. Yantorno (✉)
Centro de Investigación y Desarrollo en Fermentaciones Industriales (CINDEFI, CONICET),
Facultad de Ciencias Exactas, UNLP,
Calles 50 y 115,
1900 La Plata, Argentina
e-mail: yantorno@quimica.unlp.edu.ar

D. M. Russo · Á. Zorreguieta
Fundación Instituto Leloir, CONICET,
Patricias Argentinas 435,
C1405BWE Buenos Aires, Argentina

J. Schmitt
Synthon GmbH,
Im Neuenheimer Feld 583,
69120 Heidelberg, Germany

D. Naumann
Robert Koch-Institut,
P13, Nordufer 20,
13353 Berlin, Germany

Introduction

Bordetella pertussis is a strictly human pathogen that colonizes the respiratory tract particularly in young children, and causes whooping cough. This disease remains endemic, with incidence peaks occurring every 3–5 years, even in countries with high vaccination coverage [1, 2]. The success in host colonization requires expression of a coordinated regulation of a set of virulence factors by the bacterium that includes adhesins and toxins [3, 4] which are under the control of the *Bordetella* virulence gene activator/sensor (BvgAS) system [5]. Even though the signals that influence the BvgAS system in vivo remain unknown, Bvg-regulated gene expression can be precisely regulated in vitro. When BvgAS is active, bacteria are in the virulent (Bvg^+) phase and express a variety of virulence factors. In response to mutations or environmental signals (changes in temperature or in the concentrations of specific ions in the culture medium), *Bordetella* can switch between distinct phenotypic phases. Total inactivation of the BvgAS system results in the expression of the avirulent (Bvg^-) phenotype [6, 7].

Although vaccination has proven successful in controlling acute bacterial infection, *B. pertussis* continues to be a common cause of persistent cough in adults [8, 9]. So far little is known about the mechanism adopted by the bacteria to survive and persist in humans. Recent studies have provided evidence that bacteria of the *Bordetella* genus may undergo a community-based existence (biofilm), which might constitute a strategy for them to colonize and persist within the host [10–13]. Biofilm is a microbial lifestyle where organisms grow on surfaces in organized communities. Within biofilms, cells that are irreversibly attached to a substratum grow encased in a self-secreted heterogeneous matrix. Bacteria growing in biofilms are phenotypically different from free-floating planktonic cells [14]. Remarkably, biofilm cells are inherently more resistant to both antimicrobial agents and host defences; therefore, the formation of these sessile communities is the basis for persistency and eventual chronicity of many difficult-to-eradicate bacterial infections [15, 16].

A better understanding of biofilm development might lead to innovative effective control strategies to improve patient management. Biofilm studies are often performed using scanning electron microscopy and transmission electron microscopy [17, 18]. Electron microscope techniques require the biofilm to be dehydrated, which significantly alters its architecture [19]. To gain a better insight into the three-dimensional architecture of living, fully hydrated biofilms, confocal laser scanning microscopy (CLSM), a nondestructive technique, has been used. In the last 15 years the use of CLSM in combination with the appropriate fluorescence labels and suitable three-dimensional image software [20–22] enabled a better characterization of the physical architecture of biofilms. Qualitative and quantitative description of biofilm development is crucial for its characterization. In this regard, the COMSTAT software constitutes a computer program by which quantitative analyses of biofilm images acquired by CLSM can be performed and provides information on features such as biovolume, substrate coverage, film thickness and roughness coefficient [23].

Another task in the description of biofilm is the analysis of the macromolecular composition. Fourier transform infrared (FTIR) spectroscopy has been used as a tool for overall chemical analysis of biological samples [24–26]. The ability of FTIR spectroscopy to show the biochemical composition of sessile cells and the extracellular matrix has made this technique particularly suitable for monitoring biofilm development [26–29]. The on-line examination of microbial biofilms grown on an internal reflection element is often performed by attenuated total reflection FTIR (ATR/FTIR) spectroscopy [30]. Biofilms produced on either germanium or ZnSe internal reflection elements were studied for *Pseudomonas putida* [26], *P. aeruginosa* [28, 29], *Caulobacter crescentus* [30] and *Streptococcus pneumoniae* [27]. The spectra obtained using the aforementioned ATR/FTIR biofilm reactors contained chemical information on the sessile cells and the polymeric matrix within the first few micrometres of the depth of penetration. Although ATR/FTIR spectroscopy has demonstrated efficacy in the study of biofilm composition, two limitations of this technique should be considered: (1) the technique gives information only on the base layer of biofilms and (2) as the culture medium that circulates through biofilm water channels can also contribute to the spectral absorption, spectral subtractions of water must be continuously performed [26–28].

Recently, we applied FTIR spectroscopy to compare the phenotypic expression of *B. pertussis* cells grown adhered to abiotic surfaces with planktonic cells [11]; however, quantitative characterization of the structure *B. pertussis* mature biofilm has not been performed until now. The aim of this study was to combine data from FTIR spectroscopy, which provided in situ chemical information of biofilm development, with fluorescence microscopy images and CLSM in conjunction with the COMSTAT computer software, which allowed the quantitative characterization of three-dimensional biofilm images of *B. pertussis*. This combination enabled us to monitor the dynamics of *B. pertussis* biofilm formation and its morphological characterization in a nondestructive way.

Materials and methods

Bacterial strains and growth conditions

B. pertussis wild type, Tohama I (8132 Collection of Pasteur Institute) strain, used in vaccine production, and its derivative BP537, an avirulent Bvg$^-$ phase-locked strain [31], were used in this study. In order to perform CLSM studies, both virulent and avirulent strains were transformed with plasmid pCW505, which induces cytoplasmic expression of green fluorescent protein (GFP) without affecting growth or antigen expression [32]. Stock cultures were grown on Bordet-Gengou agar (BGA; Difco Laboratories, Detroit, USA) plates supplemented with 1% (w v^{-1}) Bactopeptone (Difco) and 15% (v v^{-1}) defibrinated sheep blood (Instituto Biológico, La Plata, Argentina) at 37 °C for 72 h, and were subcultured for 48 h. In the case of the BP537 strain, 40 μg ml^{-1} kanamicin (Sigma, St. Louis, MO, USA) was added to the culture medium.

For planktonic growth, 48-h colonies of both wild-type and Bvg$^-$ phase-locked *B. pertussis* strains, recovered from BGA plates, were transferred to 500-ml Erlenmeyer flasks containing 125 ml Stainer-Scholte (SS) medium [33], and were incubated at 37 °C on a rotatory shaker (160 rpm). Samples were taken at different time periods (lag, exponential

and stationary phases) for bacterial growth determination and IR spectroscopy studies.

B. pertussis biofilm development was studied using continuous-flow culture systems, which allowed observation and monitoring of the chemical composition in situ without disruption. For these purposes, either 0.08-mm-thick glass cover slips (20 mm×20 mm in size) or ZnSe optical plates (13 mm×2 mm, Korth Kristalle, Germany) with both sides polished were used as growth surfaces. Both types of surfaces were introduced in respective 20-ml continuous-flow chamber systems. The biofilm culture chambers were sterilized in an autoclave, except for the ZnSe windows, which were treated with 70% ethanol overnight, and were dried under a flow of sterilized air. For each assay, biofilm culture chambers were inoculated with 2 ml of a suspension of *B. pertussis* planktonic cells grown for 15 h in SS broth at 37 °C with agitation. Bacteria were allowed to attach for 4 h at 37 °C prior to the flow being initiated [11]. The sterile SS medium pumped through the flow chambers with a peristaltic pump at a flow rate of 0.1 ml min^{-1} was stirred and aerated at 37 °C. Surfaces with grown bacteria were withdrawn from the reactors at 12-, 24-, 48- and 72-h time points. Biofilms produced on cover slips were examined by fluorescence microscopy and crystal violet stain. The ones produced on ZnSe were analysed by FTIR spectroscopy (see later).

An additional study to visualize the architecture of the mature biofilm was carried out by confocal microscopy. For this, GFP-expressing *B. pertussis* cells were grown in chambered cover-glass slides containing a borosilicate glass base of 1-μm thickness (Lab-Tek Nunc; no. 155411) in SS medium at 37 °C. After 4 h of incubation, the nonattached bacteria were removed and fresh medium was added. The chambers were maintained under low agitation for 72 h in a water-saturated atmosphere to prevent desiccation.

Quantification of biofilm formation

Cells adhered to the glass surface were quantified by using a crystal violet method as described by Genevaux et al. [34] with minor modifications. Briefly, adhered biomass of each bacterial strain was evaluated after 4-h incubation (early adherence) and in the subsequent 24, 48 and 72 h of biofilm growth. Biomass adhered to glass cover slips was rinsed twice with phosphate-buffered saline (PBS) to remove unattached cells. Subsequently, adhered cells were fixed for 20 min at 80 °C. Cells were stained by addition of 0.1% crystal violet (w v^{-1}) for 5 min. After exhaustive washing, 7 ml of decolouring solution consisting of ethanol/acetone (80:20) was added to a tube containing a cover slip, and the mixture was incubated for 15 min to solubilize the stain. The absorbance of the eluted stain was measured at 590 nm (A_{590}). Good correlation between increasing total cell numbers and increasing optical density of the crystal violet stained biofilm over time was found (5×10^8 bacteria is equivalent to 0.65 absorbance units at 590 nm).

Biofilm examination by fluorescence microscopy

Biofilms developed on glass cover slips were gently washed in PBS to remove nonadhered cells and were fixed with formaldehyde 3% (v v^{-1}) for 30 min. After three washing steps with PBS, they were stained with 100 μl of aqueous acridine orange (100 mg ml^{-1}; Sigma, St. Louis, MO, USA), a fluorescent DNA dye, and were washed three times. Fluorescence microscopy was conducted with a ×100/1.25 objective under oil immersion by using a Leica DMLB microscope (Leica Microsystems, Wetzlar, Germany) equipped with a charge coupled device digital camera.

Confocal laser scanning microscopy

Biofilm architecture was studied using an inverted confocal microscope (Carl Zeiss LSM510-Axiovert 100M, Germany). Images were acquired from *B. pertussis* cells expressing GFP. The detection of the emitted fluorescence was performed by sequential scanning with settings optimal for GFP (488-nm excitation with an argon laser line and 505-nm long-pass emission). Slice images were obtained from ten random fields with a Plan-Neofluar ×100/1.3 immersion oil objective and were acquired at 1 μm *z*-intervals up through the biofilm. Therefore, ten image stacks were acquired randomly; the number of slice images in each stack varied according to the thickness of the biofilm. Simulated fluorescence projection images and vertical cross-sections through biofilms were generated using the Carl Zeiss LSM 5 Image Browser version 3.2.0 software in maximum transparency mode. In order to obtain quantitative information of the mature biofilm structure, CLSM images were analysed by the computer program COMSTAT [23], which functions under MATLAB software version 5.3 equipped with the Image Processing Toolbox. To obtain statistically representative results, quadruplicate experiments of 72-h-old biofilms of *B. pertussis* wild type and Bvg^- phase-locked mutant strains expressing GFP were performed.

FTIR spectroscopy and data analysis

ZnSe windows were removed from the chambers and gently washed three times with distilled water to remove culture medium and nonadhered cells. Then, each window was dried at 40 °C for 45 min. FTIR absorption/transmission (A/T) spectra from 4,000 to 600 cm^{-1} were acquired with a FTIR spectrometer (Spectrum One, PerkinElmer, USA) with 6-cm^{-1} spectral resolution and 64 scan co-additions. To avoid interference with spectral water vapour bands, spectra were obtained under a

continuous purge of dried air. Before data analysis, the spectra were subjected to a quality test (QT) using OPUS software. This test included a check (1) for absorbance in the amide I region (1,700-1,600 cm^{-1}) with acceptable values between 0.20 and 1.20 absorbance units, (2) for the noise signal (calculated from the first derivative between 2,100 and 2,000 cm^{-1}) with values less than 1.5×10^{-4} and (3) for the water vapour content (determined from the first derivatives between 1,847 and 1,837 cm^{-1}) with value less than 3×10^{-4}. Spectra that surpassed this QT were vector-normalized in the whole range. Four independent experiments were performed. In each experiment one ZnSe window was removed from the chambers at 24-, 48- and 72-h growth. The variance among the four independent replicates was measured by the reproducibility level (RL), which was calculated as indicated previously by Helm et al. [35]. Briefly, a cluster analysis was performed with independent replicates at each growth time. For this purpose, spectral distance values were calculated in the wavenumber range 1,200–900 cm^{-1} using the "Normal to Reprolevel" method, and the fusion value in each dendrogram was calculated by Average Linkage (OPUS, Bruker Optics, USA). The maximum spectral distance obtained in each dendrogram corresponded to the RL among replicates (OPUS working book, Bruker Optics, 2003). Spectroscopic quantification of proteins and polysaccharides was determined by means of the corresponding band-area calculations: protein content was evaluated from the amide II band area (1,590–1,480 cm^{-1}) and carbohydrate content from the carbohydrate band area (1,150–980 cm^{-1}). Derivation and band areas calculations were carried out by means of OPUS 4.0 (Bruker Optics, USA) and PerkinElmer software (Spectrum 3.0). The protein-to-carbohydrate ratio of planktonically grown cells was analysed at different stages of growth in batch cultures (lag, exponential and stationary growth phases). For this purpose, four independent cultures were performed and one sample of each growth phase was analysed in every liquid culture; thus, four independent replicates for each growth phase were analysed. Cells suspensions were washed and resuspended in sterile distilled water with an optical density at 650 nm of approximately 10. A 100-µl aliquot of each bacterial suspension was transferred to a ZnSe optical plate and dried in vacuum to obtain transparent films [36]. Absorption spectra were recorded as mentioned before. Derivation and bands-intensity calculations were carried out as mentioned before by means of OPUS 4.0 software (Bruker Optics, USA) and PerkinElmer software (Spectrum 3.0).

Statistical analysis

Four independent experiments on the three biofilm culture systems described earlier (biofilm produced on borosilicate slides, ZnSe windows and CLSM chamber) were performed. The differences in the mean values of the FTIR data were analysed by one-way analysis of variance followed by Fisher's least significant difference test.

Results and discussion

The growth in a particular niche requires bacteria to continuously monitor the surrounding conditions so as to generate an adaptive response. In general, bacteria respond to environmental conditions by controlling the expression of genes, resulting in the upregulation or downregulation of the appropriate genes. Previous works have presented evidence that most microbial cells grow in many natural and artificial habitats as biofilm [37, 38]. This type of growth produces important changes in sessile communities that eventually contribute to their pathogenicity. Current therapeutic agents, including those used for *B. pertussis*, are selected taking into account their efficacy against planktonic cells. A better understanding of the mechanisms involved in biofilm formation might be useful for devising more effective control strategies. Biofilms are difficult to study because they consist of extremely soft matter (extracellular polymeric substance) interspersed with bacteria and other materials. In this study, we propose the use of complementary techniques to evaluate *B. pertussis* growing as a sessile community.

Biofilm development

Biofilm dynamics depends on a number of different variables, including attachment of cells from the liquid phase, growth of surface-associated cells and detachment of the surface-adhered cells. In this work, the crystal violet method was used to quantify the attachment and growth of *B. pertussis* on glass cover slips contained in continuous-flow cells. Figure 1 shows the initial bacterial attachment and the time course of biomass increase. The wild-type *B. pertussis* strain reached the maximum biomass development after 48 h, with no significant changes in the following 24 h of incubation. Under the same experimental conditions, the adherence of the Bvg^- phase-locked strain was significantly lower ($P<0.01$), suggesting that the absence of Bvg-regulated factors strongly affects cell-to-surface interactions. Besides, the avirulent strain failed to grow on this surface (Fig. 1). In order to rule out the possibility that the lack of growth of the avirulent strain was due to its inability to grow in SS medium, both the wild-type and the Bvg^- phase-locked mutant strains were incubated planktonically in batch cultures in the aforementioned medium. The growth rates and the final biomass reached by both strains did not show significant differences (data not shown). Taking into account all these results, we

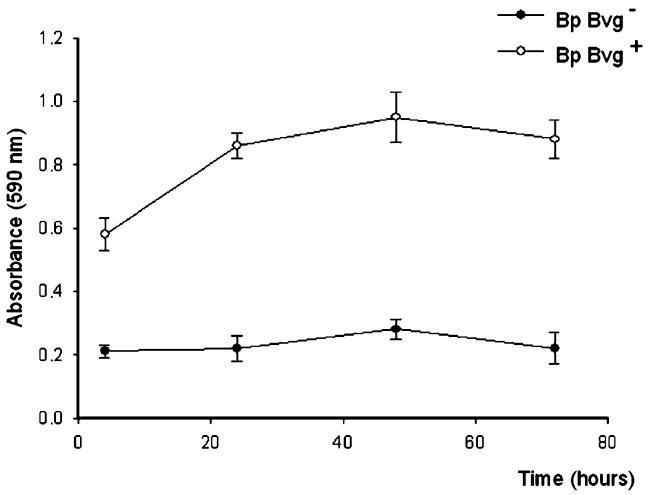

Fig. 1 Time course of biofilm formation of *Bordetella pertussis* wild-type (*Bvg*$^+$) and avirulent (*Bvg*$^-$) strains on a borosilicate surface in continuous-flow chambers. Attached biomass was stained with 0.1% crystal violet (v v^{-1}) and indirectly quantified by solubilization of the stain in alcohol/acetone (80:20). The absorbance of the resulting solution was measured at 590 nm. The data are the means ± the standard deviations of four independent experiments

suggest that the BvgAS system plays an important role in both initial attachment of *B. pertussis* and further biofilm development on this abiotic surface.

Direct examination of the different stages of *B. pertussis* biofilm growth was performed by fluorescence microscopy. As shown in Fig. 2, the presence of single cells distributed over a borosilicate surface and forming some small microcolonies was already visible after 12 h of growth in the case of the virulent strain. By day 1, small clusters of cells exceeding 50 μm in width were detected. Two days after adhesion, the biofilm appeared more structurally complex, with more than 70% of the surface of the substratum covered with large, irregularly shaped microcolonies. By day 3, the images show mature biofilms comprising large cell clusters exceeding 200 μm in width scattered over the surface. As described for other bacteria [39], we found *B. pertussis* virulent strain biofilm development to occur through different stages: (1) the initial cell attachment to a surface which takes 4 h under our experimental conditions, (2) the formation of cell aggregates (day 1) and (3) the cell proliferation and biofilm maturation (days 2–3). Figure 2 shows that under the same culture conditions, the avirulent Bvg$^-$ phase-locked strain failed to grow and develop a mature biofilm. Only a few single cells attached to the surface 12 h after inoculation could be seen. These adhered cells exhibited neither a marked increase of biomass nor progress in the development of microcolonies over time. Mishra et al. [13] proposed that biofilm development in *B. bronchiseptica* is characterized by an initial Bvg-independent step (attachment) and a subsequent Bvg-dependent step. However, our results clearly demonstrated that in the case of *B. pertussis* biofilm formation both the attachment and the biofilm development are dependent on one or more of the virulence factors under the regulation of the Bvg system.

Characterization of biofilm architecture

To further characterize the structure of *B. pertussis* mature biofilm, CLSM was used to image the biofilm produced by GFP-expressing *B. pertussis* cells. An argon laser at 488 nm was used to excite the GFP; the fluorescence emitted by the GFP-tagged bacteria was monitored with a 505-nm long-pass emission filter. Figure 3 depicts the spatial biomass distribution on glass surfaces of virulent

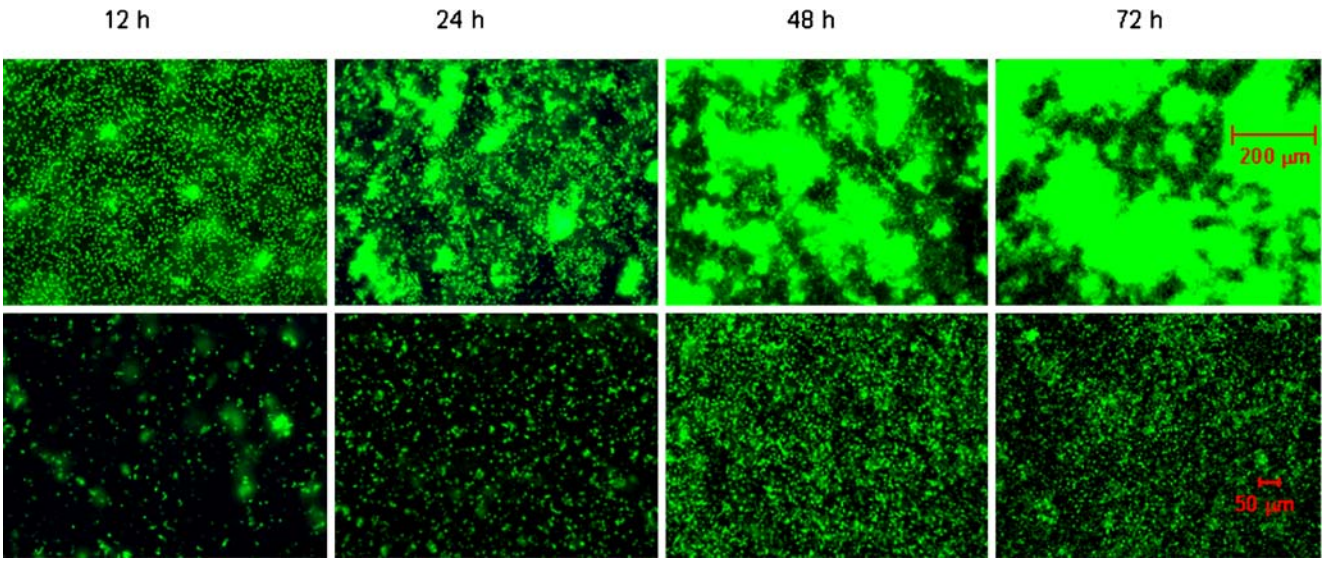

Fig. 2 Epifluorescence microscopy micrographs from different stages of biofilm formation over 72 h. *B. pertussis* wild-type (*top panels*) and Bvg$^-$ phase-locked (*bottom panels*) strains were grown on glass cover slips in continuous-flow chambers, fixed with formaldehyde 3% (v/v) and stained with acridine orange for microscopic observation. Images were obtained with a ×100/1.25 immersion oil objective

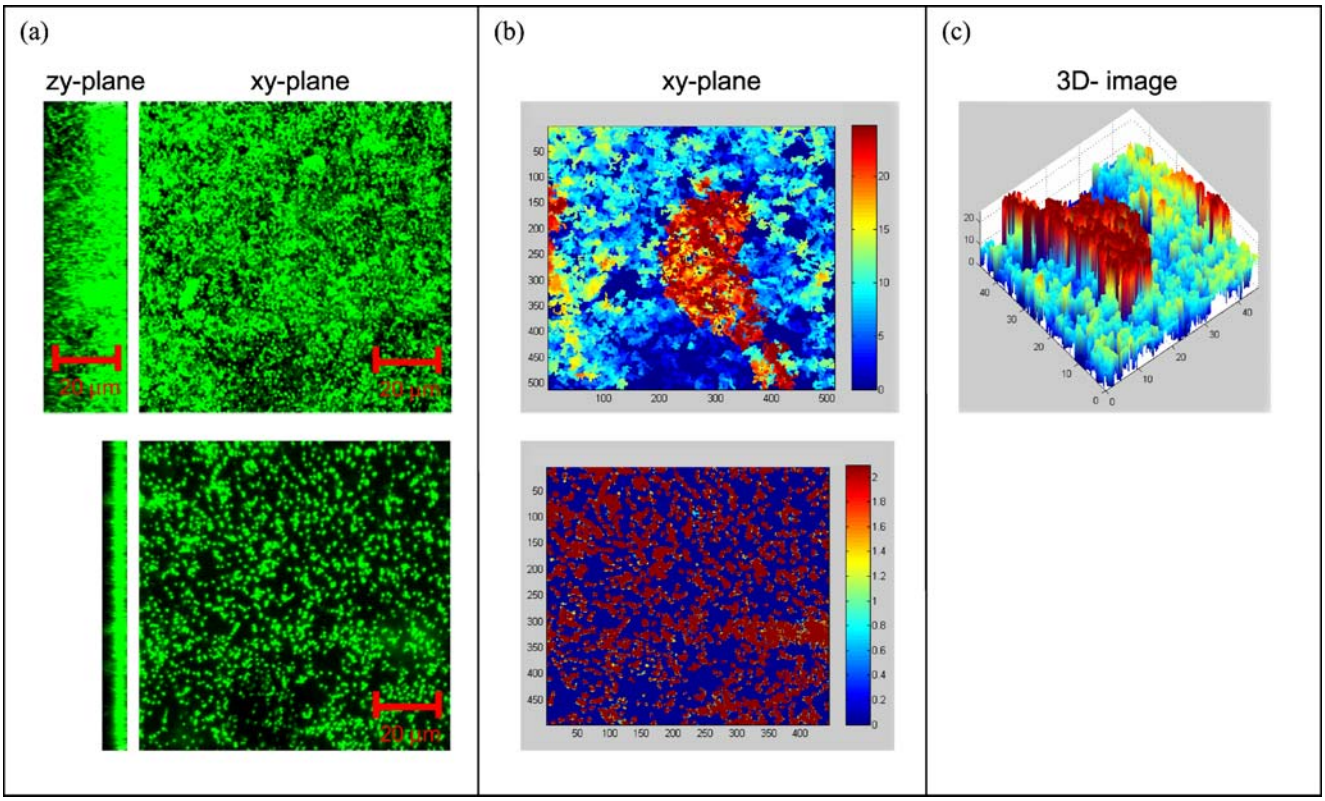

Fig. 3 Confocal laser scanning microscope images of *B. pertussis* biofilms. Biofilms of wild-type (*top panels*) and Bvg$^-$ phase-locked (*bottom panels*) strains of *B. pertussis* containing the green fluorescent protein expressing plasmid pCW505, were grown on chambered cover glass slides containing a borosilicate glass base of 1-µm thickness for 72 h. **a** Images represent superimposed horizontal (*xy*-axis) and vertical (*zy*-axis) optical sections taken with a distance of 1 µm between them. Images were reconstructed using LSM Image Browser version 3.2.0 in maximum transparency mode. The *scale bars* represent 20 µm. **b** *xy*-axis intensity map reflecting biofilm thickness (microns) and **c** three-dimensional view of the intensity map (*xyz*) showing biofilm thickness. The images in **b** and **c** were obtained with the computer program COMSTAT [23] under MATLAB version 5.3 software. The *colour scale* in **b** and **c** represents the depth coding of the level from the surface

(Fig. 3, top panel) and avirulent (Fig. 3, bottom panel) strains after 72 h of incubation. The micrographs show that while the wild-type strain uniformly covered the surface forming a structured biofilm composed of cell clusters, the Bvg$^-$ phase-locked strain failed to form this biofilm (Fig. 3a, *xy*-plane). A further observation associated with the development of a mature biofilm by the wild-type strain was the presence of water channels (Fig. 3a, *zy*- and *xy*-planes). Figure 3b and c shows an intensity map of the wild-type (top panels) and mutant strain (bottom panel) biofilms, which shows, through a colour scale, the differences in biofilm thickness. These images were obtained by the computer program COMSTAT [23] working under MATLAB software version 5.3 equipped with the Image Processing Toolbox. The thickness distribution was determined according to the method of Heydorn et al. [23]. COMSTAT software was also used in order to obtain a detailed, accurate and objective structural biofilm comparison between the wild-type and the Bvg$^-$ phase-locked mutant biofilms. Six parameters for biofilm architecture characterization were determined (Table 1). Significant differences between the two strains were found in most of the parameters evaluated. First of all, colonization of the substratum by the wild-type strain was significantly higher in 72-h-old biofilm than that calculated for the avirulent strain (substratum coverage of 72 versus 25%). The high value (1.18±0.09) found for the roughness coefficient in the growth of the avirulent strain on cover slips is an evident indication that the Bvg$^-$ phase-locked strain formed

Table 1 Quantitative analysis of the structure of biofilm formed by *Bordetella pertussis* wild-type (Bp Tohama I) and Bvg$^-$ phase-locked (Bp 537) strains grown on 1-µm-thick cover slips contained in chambers for 72 h

Quantitative parameters	Bp Tohama I (wt)	Bp 537 (Bvg$^-$)
Mean thickness (µm)	8.47 (0.21)	0.82 (0.04)
Maximum thickness (µm)	24.75 (0.45)	2.10 (0.29)
Biovolume	2.93 (0.24)	0.86 (0.05)
Substrate coverage	0.72 (0.12)	0.25 (0.03)
Surface-to-volume ratio ($\mu m^2\ \mu m^{-3}$)	7.28 (0.38)	7.83 (0.54)
Roughness coefficient	0.69 (0.07)	1.18 (0.09)

Parameters correspond to mean values of four replicates. Standard errors are indicated in *parentheses*.

a flat, uniform and unstructured biofilm lacking water channels. The total biovolume of the wild-type biofilm was almost 3.5-fold higher than that of the Bvg$^-$ phase-locked strain biofilm, confirming that the wild-type strain biofilm contains the greater biomass. The wild-type biofilm had a maximum thickness of approximately 24 μm, which was significantly higher than the value obtained for avirulent cells attached to cover slips (approximately 2 μm). Interestingly, while the maximum thickness of *B. pertussis* biofilm was almost 24 μm, that of mature biofilms of other respiratory pathogens like *S. pneumoniae* [40] or *P. aeruginosa* [28], developed under similar conditions, was 150 and 120 μm, respectively. These variations illustrate specific modes of growth of bacteria adhered to surfaces of different organisms.

Monitoring of biofilm development by FTIR spectroscopy

In order to gain chemical information on the different stages of biofilm formation of *B. pertussis* in a nondestructive manner, we applied a continuous-flow cell system where bacteria were grown adhered to ZnSe windows as a substratum. Figure 4 shows FT-IR A/T spectra of *B. pertussis* wild-type strain obtained at different time points during growth on ZnSe. The spectra represent one of the four independent replicates obtained at different times of growth. The variance among replicates, determined by the RL, was 12, 10 and 15, at 24, 48 and 72 h, respectively. IR bands intensities associated with specific biomass markers such as lipids (fatty acid region, 3,000–2,800 cm^{-1}), carbohydrates (1,200–900-cm^{-1} region) and proteins (amide I and II, 1,650 and 1,540 cm^{-1}, respectively) [35, 36] increased over the first 2 days of incubation, indicating accumulation of sessile cells on the substratum (Fig. 4, Table 2). Particularly, the intensities of the specific carbohydrate bands at 1,100 and 1,020 cm^{-1} (due to C–OH stretching modes and C–O–C and C–O ring vibrations) [25, 26, 28, 35, 36], and a band around 800 cm^{-1} (assigned to the glycosidic linkage type) [41] vary considerably over the duration of the experiment. Other bands also observed in *P. aeruginosa* biofilms and assigned to its matrix [25] were found to increase during the 72 h of growth in *B. pertussis* biofilm: a band at 1,733 cm^{-1} (assigned to C=O stretching of esters), a peak at 1,375 cm^{-1} (symmetric stretching of the carboxylate ion) and a band at 1,260 cm^{-1} (C–O–C of esters). These results provided evidence that polysaccharides with *O*-acetyl groups were present within *B. pertussis* wild-type strain biofilm. Besides, an increase in band intensities at 2,920 and 2,850 cm^{-1} (assigned to >CH_2 asymmetric and symmetric stretching of fatty acids, respectively), a weak band at 1,450 cm^{-1} (C–H bending of CH_2) and a band at 720 cm^{-1} (C–H rocking of >CH_2 methylene) [34], most

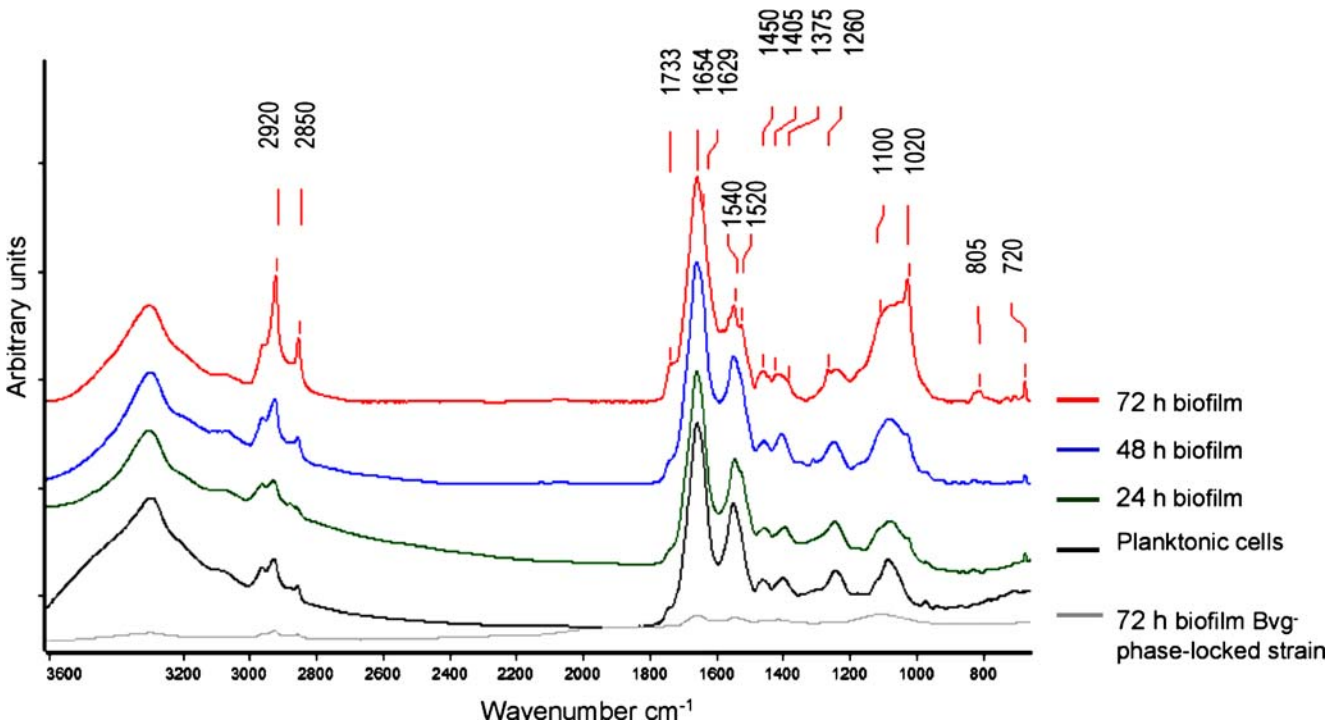

Fig. 4 Normalized Fourier transform IR absorption/transmission spectra of *B. pertussis* wild-type strain obtained at different time points during biofilm growth (24, 48 and 72 h) and *B. pertussis* Bvg$^-$ phase-locked strain over 72-h incubation (*grey line*), cultivated on ZnSe windows in continuous-flow cells. The spectrum of the Bvg$^-$ cells did not surpass the quality test (amide I absorbance less than 0.2), so it was not vector-normalized. *B. pertussis* wild-type strain grown planktonically in Stainer-Scholte medium (exponential phase) is indicated by the *black line*

Table 2 Protein-to-carbohydrate content evaluated by Fourier transform IR spectroscopy

Type of culture	Phase growth or incubation time	Proteins (amide II)	Carbohydrates ($1{,}200–900\text{-cm}^{-1}$ region)	Carbohydrates/proteins[a]
Batch	Lag (~2 h)	15.36 (0.42)	7.95 (0.29)	0.52 (0.03) AB
	Exponential (~15 h)	14.27 (0.47)	6.99 (0.32)	0.49 (0.02) AC
	Stationary (~30 h)	12.95 (0.45)	9.34 (0.35)	0.72 (0.04) B
Biofilm	24 h	1.58 (0.02)	1.41 (0.03)	0.89 (0.03) D
	48 h	1.64 (0.02)	2.08 (0.04)	1.27 (0.02) E
	72 h	1.16 (0.04)	3.58 (0.09)	3.09 (0.12) F

[a] Ratio of the band areas assigned to protein absorption (amide II, 1,590–1,480 cm^{-1}) and carbohydrates (1,145–980 cm^{-1}). Data are reported as averages and standard errors (in *parentheses*) of four separate experiments. Significant differences between carbohydrate-to-protein ratios are indicated by different *letters* and were determined using Fisher's least significant difference test at the 5% level after a one-way analysis of variance.

B. pertussis wild-type cells were cultivated planktonically in batch cultures and as biofilm in a cell flow chamber on ZnSe windows.

possibly due to lipopolysaccharides [11], were detected for biofilm growth over time. These results could indicate a progressive accumulation of lipopolysaccharides in the matrix during biofilm formation.

Table 2 shows the protein and carbohydrate contents, evaluated by FTIR spectroscopy, for *B. pertussis* wild-type strain grown both planktonically in batch culture (different phases of growth) and as biofilm under continuous-flow conditions on ZnSe windows. IR band areas associated with carbohydrate absorptions increased at a substantially higher rate than that of the amide II band, which can be associated with the production of the extracellular polymeric substance during biofilm development as previously reported [11]. Carbohydrate-to-protein ratios increased almost 3.5 times during biofilm growth in the course of the experiment, and they were significantly higher than the ratios found for the different phases of planktonically grown cells (Table 2). Interestingly, these results are in agreement with those reported by Donlan et al. [27] for *S. pneumoniae* biofilm.

In contrast to the results found for the *B. pertussis* wild-type strain, the avirulent cells almost failed to grow adhered on ZnSe windows. Only very weak bands were detected after 72 h of incubation (the amide I band absorbance was less than 0.2) (Fig. 4). Figure 4 also shows the IR spectrum of *B. pertussis* wild-type cells grown planktonically in SS medium, which was included as a control experiment to demonstrate that the aforementioned bands are characteristic of the mode of growth of the biofilm.

It is important to mention the fact that the physical characteristics of the dried biofilms obtained on ZnSe windows allowed the acquisition of relatively good quality spectra using the A/T mode. While ATR/FTIR spectroscopy allows spectra containing the chemical information of a thin layer adjacent to the crystal surface (1-2-μm penetration depth) to be obtained, spectra obtained using the A/T mode of operation provide information on the total composition of the sessile cells and the polymeric matrix throughout the whole biofilm. Thus, the system described in this work is suitable for detecting biochemical changes during *B. pertussis* biofilm formation over time.

The results regarding the biofilm development obtained by FTIR spectroscopy can be correlated with the fluorescence microscopy images. Wild-type bacteria formed strong biofilms that resulted in large, irregularly shaped microcolonies scattered over the surface (Fig. 2). As found by FTIR spectroscopy the development of these structures was related to an increase in the carbohydrate-to-protein ratio. Thus, the progress towards a mature biofilm in *B. pertussis* might be associated with the production of a polysaccharide-enriched matrix, which contributes to the biofilm architecture.

Notably, while fluorescence microscopy showed an apparent increase of biomass during the course of the experiments (72 h) (Fig. 2), the crystal violet absorption by cells adhered to surfaces increases in the first 48 h of incubation, with no significant changes in the following 24 h (Fig. 1). On the other hand, the FTIR spectroscopy results showed that the amide II band area decreased after 48 h of growth (Fig. 4). The measurements from IR spectroscopy in A/T mode reflect the total biofilm composition (biomass and extracellular matrix). Since the matrix protein content is less than 8% (w w^{-1}) as we previously reported [11], one could speculate that the reduction in the amide II band area could be attributed to a partial detachment of the bacteria adhered to ZnSe windows.

Conclusions

In the present work several complementary techniques were successfully applied to characterize the development of *B. pertussis* biofilm. Using these techniques, we demonstrated that the attachment, growth of surface-associated cells and the development of mature biofilm were dependent on the expression of virulence factors regulated by the BvgAS system. Fluorescence microscopy images demon-

strated that the biofilm formation in *B. pertussis* occurs in stages. Quantitative analysis of CLSM images performed with COMSTAT image analysis software allowed quantitative numbers on mature biofilm morphology to be accumulated. By means of FTIR spectroscopy, it was demonstrated that biofilm growth is accompanied by significant changes in carbohydrate expression level, providing a link between the polysaccharide overproduction and the *B. pertussis* biofilm maturation. The combination of these techniques yielded complementary results that allowed improved characterization of virulent *B. pertussis* biofilm development. These techniques might be a useful tool for a better understanding of biofilm growth and persistence within the host. The analytical approach proposed in this work could also be used to address the role of individual virulence factors, antimicrobial agents and shear stress in the development and persistence of this pathogen grown on surfaces. These results might also have direct implications for the design of new preventive or therapeutic strategies.

Acknowledgements This work was supported by a grant from Secretaría de Ciencia y Técnica, Argentina, PICT 98-06-03824. O.Y. is Professor of UNLP; M.E.R. and A.Z. are members of the Scientific Career of CONICET; A.B. is a member of the CIC PBA; D.S. and D. M.R. are doctoral fellows of CONICET and Fundación Antorchas, respectively.

References

1. Mooi FR, van Loo IH, King AJ (2001) Emerg Infect Dis 7:526–528
2. Qiushui H, Makinen J, Berbers G, Mooi FR, Viljanesn MK, Arvilommi H, Mertsola J (2003) J Infect Dis 187:1200–1205
3. Cotter PA, Yuk MH, Mattoo S, Akerley BJ, Boschwitz J, Relman DA, Miller JF (1998) Infect Immun 69:5921–5929
4. Mattoo S, Miller JF, Cotter PA (2000) Infect Immun 68:2024–2033
5. Stibitz S, Aaronson W, Monack D, Falkow S (1989) Nature 338:266–269
6. Arico B, Scarlato V, Monack DM, Falkow S, Rappuoli R (1991) Mol Microbiol 5:2481–2491
7. Lacey BW (1960) J Hyg 58:57–93
8. Cherry JD, Grimprel E, Guiso N, Heininger U, Mertsola J (2005) J Pediatr Infect Dis 24:S25–S34
9. Mattoo S, Cherry JD (2005) Clin Microbiol Rev 18:326–382
10. Bosch A, Massa NE, Donolo AS, Yantorno O (2000) Phys Status Solidi B220:635–640
11. Bosch A, Serra D, Prieto C, Schmitt J, Naumann D, Yantorno O (2006) Appl Microbiol Biotechnol 71:736–742
12. Irie Y, Mattoo S, Yuk MH (2004) J Bacteriol 186:5692–5698
13. Mishra M, Parise G, Jackson KD, Wozniak DJ, Deora R (2005) J Bacteriol 187:1474–1484
14. Donlan RM (2002) Emerg Infect Dis 8:881–890
15. Costerton JW, Montanaro L, Arciola CR (2005) Int J Artif Organs 28:1062–1068
16. Fux CA, Costerton JW, Stewart PS, Stoodley P (2005) Trends Microbiol 13:34–40
17. Danilatos GD (1993) Microsc Res Tech 25:354–361
18. Koval SF, Beveridge TJ (1999) In: Lederberg J (ed) Encyclopedia of microbiology. Academic, San Diego, pp 276–287
19. Geesey GG, Richardson WT, Yeomans HG, Irvin RT, Costerton, JW (1977) Can J Microbiol 23:1733–1736
20. Bloemberg GV, O'Toole GA, Lugtenberg BJJ, Kolter R (1997) Appl Environ Microbiol 63:4543–4551
21. Lawrence JR, Korber DR, Hoyle BD, Costerton JW, Caldwell DE (1991) J Bacteriol 173:6558–6567
22. Nancharaiah YV, Venugopalan VP, Wuertz S, Wilderer PA, Hausner M (2005) J Microbiol Methods 60:179–187
23. Heydorn A, Nielsen AT, Hentzer M, Sternberg C, Givskov M, Ersbøll, BK, Molin S (2000) Microbiology 146:2395–2407
24. Naumann D, Helm D, Labischinski H (1991) Nature 351:81–82
25. Nichols P, Henson J, Guckert J, Nivens D, White D (1985) J Microbiol Methods 4:79–94
26. Schmitt J, Nivens D, White DC, Flemming HC (1995) Water Sci Technol 32:149–155
27. Donlan RM, Piede JA, Heyes CD, Sanii L, Murga R, Edmonds P, El Sayed I, El Sayed MA (2004) Appl Environ Microbiol 70:4980–4988
28. Nivens DE, Ohman DE, Williams J, Franklin MJ (2001) J Bacteriol 183:1047–1057
29. Suci PA, Mittelman MW, Yu FP, Geesey GG (1994) Antimicrob Agents Chemother 38:2125–2133
30. Nivens D, Chambers JQ, Anderson TR, Tunllid A, Shmitt J, White DC (1993) J Microbiol Methods 17:199–213
31. Relman D, Tuomanen E, Falkow S, Golenbock, DT, Saukkonen K, Wright SD (1990) Cell 61:1375–1382
32. Weingart CL, Broitman-Maduro G, Dean G, Newman S, Peppler M, Weiss AA (1999) Infect Immun 67:4264–4273
33. Stainer DW, Scholte MJ (1971) J Gen Microbiol 63:211–220
34. Genevaux P, Muller S, Bauda P (1996) FEMS Microbiol Lett 142:27–30
35. Helm D, Labischinski H, Schallehn G, Naumann D (1991) J Gen Microbiol 137:9–79
36. Naumann D (2000) Infrared spectroscopy in microbiology. Wiley, Chichester, pp 1–29
37. Costerton JW, Stewart PS, Greenberg EP (1999) Science 284:1318–1322
38. Donlan RM, Costerton JW (2002) Clin Microbiol Rev 15:167–193
39. Sauer K, Camper AK, Ehrlich GD, Costerton JW, Davies DG (2002) J Bacteriol 184:1140–1154
40. Allegrucci M, Hu FZ, Shen K, Hayes J, Ehrlich GD, Post JC, Sauer K (2006) J Bacteriol 188:2325–2335
41. Synytsya A, Copíková J, Matejka P, Machovic V (2003) Carbohydr Polym 54:97–106